Acta Crystallographica Section D
Biological Crystallography
ISSN 0907-4449

The three-dimensional structure of cytosolic bovine retinal creatine kinase

Dominic Tisi,[a]† Ben Bax[a]‡ and Andreas Loew[b]*

[a]Department of Crystallography, Birkbeck College, Malet Street, London WC1 7HX, England, and [b]Department of Biochemistry, Southwestern Medical Center, University of Texas, 5323 Harry Hines Boulevard, Dallas, TX 75390-9050, USA

† Present address: Astex, 250 Cambridge Science Park, Milton Road, Cambridge CB4 0WE, England.
‡ Present address: SmithKline Beecham Pharmaceuticals, New Frontiers Science Park (North), Third Avenue, Harlow, Essex CM19 5AW, England.

Correspondence e-mail: aloew@chop.swmed.edu

Received 26 June 2000
Accepted 27 October 2000

PDB Reference: cytosolic bovine retinal creatine kinase, 1g0w.

Creatine kinase (CK) catalyses the reversible transfer of the phosphate moiety from phosphocreatine (PCr) to ADP, generating creatine and ATP. The crystal structure of a cytosolic brain-type creatine kinase is reported at 2.3 Å. The biological dimer sits on a crystallographic twofold axis. The N-terminal residues of both subunits come very close to the crystallographic twofold at the dimer interface. The electron density observed is consistent with two alternative conformations for the N-termini, as previously found for chicken brain-type creatine kinase.

1. Introduction

Members of the family of structurally and functionally related ATP:guanidino phosphotransferases (Lehninger, 1992; Watts, 1971) reversibly catalyse the transfer of phosphate between ATP and various phosphagens, thereby maintaining constant levels of ATP in the cell. Creatine kinase (CK; E.C. 2.7.3.2) is a member of this enzyme class and catalyses the reversible phosphoryl-transfer reaction between phosphocreatine (PCr) and ADP. Most invertebrates have arginine kinase (AK) as their sole guanidino kinase (Watts, 1971; Ellington, 1989). This enzyme performs a similar function to creatine kinase in that it produces high-energy phosphagens (phosphoarginine; PAr) for use in energy-requiring processes,

$$\mathrm{PCr} + \mathrm{Mg\text{-}ADP} + \mathrm{H^+} \leftrightarrow \mathrm{Cr} + \mathrm{Mg\text{-}ATP}$$
$$\mathrm{PAr} + \mathrm{Mg\text{-}ADP} + \mathrm{H^+} \leftrightarrow \mathrm{Ar} + \mathrm{Mg\text{-}ATP}.$$

Four isoforms of creatine kinase exist which are categorized by their sub-cellular localization (Eppenberger *et al.*, 1967; Jacobus & Lehninger, 1973). There are two cytosolic isoforms, brain type (B) and muscle type (M), which can form homodimers or heterodimers (MM, BB, MB). The two mitochondrial isoforms, a striated muscle-specific isoform ($\mathrm{Mi_b}$-CK; b for basic) and a so-called 'ubiquitous' isoform ($\mathrm{Mi_a}$-CK; a for acidic), are located exclusively in the intermembrane compartment of the mitochondria (DeLuca & Hall, 1980). These mitochondrial isoforms form octamers comprised of four stable dimers (Schlegel *et al.*, 1988; Belousova *et al.*, 1991).

Sequence analysis of the guanidino kinase family shows a highly conserved protein family (Muhlebach *et al.*, 1994). Members of the cytosolic CKs exhibit 77–82% sequence identity and the mitochondrial isoforms show 82–85% sequence identity. Cytosolic and mitochondrial isoforms show 60–66% sequence identity, while a comparison of CK and AK sequences shows 38–44% identity. Sequence analysis of CK isoforms has identified six highly conserved regions flanked by

Table 1
Data collection and refinement statistics.

Values in parentheses indicate the corresponding values for the completeness, multiplicity and R_{merge} in the outer shell for data set *A* (2.8–2.7 Å) and data set *B* (2.4–2.3 Å).

Data set (resolution)	*A* (2.7 Å)	*B* (2.3 Å)
Space group	$P4_32_12$	$P4_32_12$
Unit-cell parameters *a*, *b*, *c* (Å)	96.2, 96.2, 108.1	95.6, 95.6, 107.9
Wavelength (Å)	1.54	0.89
Unique reflections	14578	18573
Completeness (%)	99 (98.7)	96.8 (95.8)
Multiplicity	3.8 (3.8)	3.7 (3.6)
R_{merge}	5.6 (16.6)	8.4 (22.2)

seven more variable sections. These six conserved regions are collectively termed the 'CK framework' and are responsible for basic enzyme function. The more variable regions are believed to be involved in isoenzyme-specific functions such as oligomerization (Hossle *et al.*, 1988).

Both mitochondrial and cytosolic CK isoforms are functionally coupled to sites of energy utilization and production (Wallimann *et al.*, 1984; Wegmann *et al.*, 1992). The close association of Mi-CK, porin and adenine nucleotide translocase (Beutner *et al.*, 1996) might provide direct access for Mi-CK to mitochondrial matrix-generated ATP. This protein complex also provides a route for Mi-CK generated PCr into the cytosol. The shuttling of PCr from the mitochondria into the cytosol is the basis of the phosphocreatine circuit/shuttle. This provides a mechanism of energy homeostasis in which both mitochondrial and cytosolic CK isoforms play a pivotal role (Wallimann *et al.*, 1992).

Although the CK family has been subjected to extensive biochemical investigation, a definitive mechanism of phosphoryl transfer has yet to be elucidated. Small-angle scattering studies (Forstner *et al.*, 1996) using dimeric rabbit muscle creatine kinase identified a large reduction in the radius of gyration (28.0–25.5 Å) upon substrate binding, suggesting a substantial degree of conformational change. Several residues and peptide regions have been implicated in catalysis. For example, lysine and arginine residues have been proposed to interact with the negatively charged phosphate groups of ADP/ATP (Bose & Friedberg, 1971; James & Cohn, 1974; Borders & Riordan, 1975; Wood *et al.*, 1998). A tryptophan residue is suspected to form a stack with the adenine base moiety (Vasak *et al.*, 1979; Gross *et al.*, 1994). The highly conserved cysteine (Cys283) has also been implicated in catalysis, as chemical modification with a variety of reagents leads to full or partial inactivation of the enzyme (Watts, 1973; Buechter *et al.*, 1992). More recently, the role of the conserved cysteine was proposed to function more in the synergism of substrate binding than directly in catalysis (Furter *et al.*, 1993).

Only when the X-ray structures became available did a comparison of the cytosolic isoenzymes (Rao *et al.*, 1998; Eder *et al.*, 1999) with structures of octameric mitochondrial CK isoforms (Fritz-Wolf *et al.*, 1996; Eder *et al.*, 2000) and horseshoe crab arginine kinase (hc-AK) complexed with a transition-state analogue (Zhou *et al.*, 1998) allow a more definitive identification of residues involved in substrate binding and catalysis. Arginine kinase and creatine kinase both perform the same function, reversible phosphoryl transfer. Both enzymes utilize adenine nucleotides (ATP/ADP) and the phosphoryl acceptors only differ slightly (Cr/PCr and Ar/PAr). Owing to the sequence and functional similarities of the arginine and creatine kinases, the structure of hc-AK provides a template from which those residues are likely to form the nucleotide and creatine-binding sites can be identified. The amino-acid differences between hc-AK and brB-CK localized at the active site complement the different substrate specificities of the two guanidino kinases.

2. Materials and methods

2.1. Purification and crystallization

Bovine retinal brain-type creatine kinase (brB-CK) was purified from bovine photoreceptor cells and crystallized as described by Loew & Bax (1998). Crystals were also grown at a higher temperature (293 rather than 277 K); attempts to grow crystals of a transition-state complex of brB-CK have not to date been successful.

2.2. Data collection and processing

The collection of a 2.7 Å data set on a MAR Research imaging plate mounted on a GX-21 rotating-anode generator has been described (Loew & Bax, 1998); the images of this 2.7 Å data set were reprocessed with *DENZO* (Otwinowski & Minor, 1997) to give data set *A* (Table 1). Data set *B*, extending to higher resolution (2.3 Å), was subsequently collected from a single unfrozen crystal on station 9.5 at the SRS, Daresbury. The 2.7 Å data set did not scale well with the 2.3 Å data set; there were small differences in unit-cell parameters.

Frozen crystals (frozen from a cryosolution of 100 m*M* HEPES pH 7.5, 2.4 *M* ammonium sulfate, 25% glycerol) typically have very high mosaic spread and have not to date yielded good quality data.

2.3. Structure determination

The structure was determined by molecular replacement using the 2.7 Å data set (data set *A*; prior to the collection of data set *B*). The search model was subunit *A* from the structure of octameric chicken mitochondrial creatine kinase (Mi_b-CK; PDB code 1crk; Fritz-Wolf *et al.*, 1996). The percentage sequence identity between the amino-acid sequences of brB-CK and Mi_b-CK is 65% and this, together with the fact that there is only a single subunit of brB-CK in the asymmetric unit, made the molecular replacement straightforward. The rotation and translation functions were determined with *AMoRe* (Navaza & Saludjian, 1997) as implemented in the *CCP*4 suite of programs (Collaborative Computational Project, Number 4, 1994). The rotation function calculated with data between 15 and 3.5 Å yielded a clear solution (height 19.30σ, compared with a first noise peak of

9.95σ). Translation functions were calculated in both $P4_32_12$ and $P4_12_12$; a clear solution was obtained in $P4_32_12$ with a correlation coefficient of 58.5 (38.9) and an R factor of 43.5% (51.7%) (numbers in parentheses are the correlation coefficient and R factor of the first noise peak). In comparison, in $P4_12_12$ the highest peak had a correlation coefficient of 30.1 (27.3) and an R factor of 49.3% (50.5%), clearly indicating that the correct space group was $P4_32_12$.

2.4. Refinement against the 2.7 Å data set

The chicken creatine kinase subunit was positioned in the $P4_32_12$ cell of the brB-CK crystal by rotating it and translating it with *PDBSET* (Collaborative Computational Project, Number 4, 1994) as indicated by the molecular-replacement solution. In an initial round of refinement with *CNS* (Brunger *et al.*, 1998), the model was first subjected to 40 cycles of rigid-body refinement as a single subunit and to the refinement of an overall temperature factor. This initial refinement was followed by refinement of the protein as two rigid bodies corresponding to the two domains (residues 1–112 and 113–380) identified by Fritz-Wolf *et al.* (1996). This reduced the R factor and free R factor to 36.9 and 39.1%, respectively. Five rounds of rebuilding with the computer graphics program *O* (Jones *et al.*, 1991) then followed, followed by refinement with *CNS* (Brunger *et al.*, 1998). Each refinement round included bulk-solvent scaling, anisotropic temperature-factor refinement and 120 cycles of restrained positional refinement. In the first round of rebuilding, side chains which differed between brB-CK and chicken Mib-CK were replaced and several regions with poor density were omitted. After five rounds of rebuilding and refinement, the R factor and free R factor had dropped to 21.8 and 28.3%, respectively. Extensive rebuilding had been carried out on several regions of the molecule (including residues 98–105, 300–330 and 365–380) and there was good $2F_o - F_c$ density for almost the entire model. At this stage in the refinement, the 2.3 Å data set was introduced and refinement was continued against this data set.

2.5. Refinement against the 2.3 Å data set

The brB-CK model from the 2.7 Å refinement was subject to 50 cycles of rigid-body refinement against the 2.3 Å data set. Nine further cycles of rebuilding (with *O*) and refinement (with *CNS*) reduced the R factor and $R_{\rm free}$ to 21.5 and 28.0%, respcetively. Two prominent peaks of electron density in the active site were modelled as sulfate ions (1.9 *M* ammonium sulfate was present in the crystallization buffer). The model at this stage included two sulfates, 35 water molecules and residues 11–380 of creatine kinase. The density for all residues was reasonable, except for residues 320–329, which had weak density throughout the refinement and appear to be largely disordered. Density close to Cys283 (near the active site) was not well modelled as a water molecule and suggested the presence of a covalent adduct on the cysteine. This was modelled as a thioester-linked creatine attached to the cysteine.

2.6. Unexplained density on the twofold axis of the creatine kinase dimer

Cytosolic creatine kinases, such as brB-CK, are dimeric. In the crystal structure of brB-CK described here the creatine kinase dimer sits on a crystallographic twofold axis running along the *ab* diagonal of the cell.

Throughout the refinement of the structure of brB-CK we observed two prominent peaks (in $F_o - F_c$ maps) on the crystallographic twofold axis relating the two subunits in the brB-CK dimer. There is other weaker density between Lys11 (the last residue for which we have unambiguous density) and these two prominent peaks of density on the twofold axis, suggesting that the N-termini of the two symmetry-related subunits in the dimer may lead in this direction. This density does not seem to be an artefact since it is present in both the 2.7 and 2.3 Å data sets and is not the function of a few reflections with large $F_o - F_c$ differences.

In order to try and interpret this density the following were performed. (i) Further rounds of refinement were carried out with *REFMAC* (Murshudov *et al.*, 1999) and *CNS* (Brunger *et al.*, 1998). (ii) A cDNA coding for bovine brain-type creatine kinase was sequenced (see below) and as a consequence nine side chains were changed. (Note our previous interpretation had relied on amino-acid sequences of dog brain-type creatine kinase and human brain-type creatine kinase, which share some 97% identity with bovine brain-type creatine kinase). (iii) An automated refinement procedure, *ARP* (Perrakis *et al.*, 1999), was also used in a script which incorporated *REFMAC* to try and produce an unbiased map. (iv) When the coordinates of chicken cytosolic brain-type creatine kinase became available (Eder *et al.*, 1999), we re-solved the structure by molecular replacement, confirming our previous model. Furthermore, since chicken cytosolic brain-type creatine kinase crystallizes in $P2_1$ with two homodimers per asymmetric unit, we were able to extend our previously unsolved density on the crystallographic twofold by building alternate N-terminal conformations based on the chicken brain-type creatine kinase structure. It appears therefore that the most probable explanation for this extra density is that the N-terminus of each monomer has two conformations lying between the two subunits in the dimer. The observed density would thus be an average of two such N-termini per monomer, related by the crystallographic twofold axis, each with an occupancy of 0.5. The resulting N-termini of the creatine kinase dimer therefore occupy distinct but different conformations (similar to the N-termini observed in the recently reported structure of the cytosolic chicken brain-type creatine kinase; Eder *et al.*, 1999).

2.7. Final coordinates

The final coordinates consist of residues 12–381 (excluding residues 322–329, which are disordered), two sulfate ions with full occupancy (in the active site), alternate conformations for residues 2–11 with occupancy 0.5 (on the crystallographic twofold) and 65 waters. The R factor and $R_{\rm free}$ are 18.6 and

22.8, respectively, for all data in the resolution range 10.0–2.3 Å (including a bulk-solvent correction).

2.8. Sequence of bovine brain-type creatine kinase

Cloning of bovine brain-type creatine kinase was performed using a one-step room-temperature polymerase chain reaction (RT-PCR) with poly(A)+ mRNA as a template. Briefly, 1 ng bovine retinal poly(A)+ mRNA (kindly provided by Dr Federico Gonzalez-Fernandez, University of Virginia, USA) was used in a TITAN one-tube RT-PCR reaction according to the manufacturer's suggestion (Roche Molecular Biochemicals, Indianapolis, IN, USA). The 5′-primer was designed based on a partial N-terminal protein sequence obtained by Edman degradation of a purified brB-CK sample (5′-primer used in RT-PCR reaction: 5′-ATGCCCTTCTCCAACAG). The 3′-primer was generated by DNA-sequence alignments of all known brain-type creatine kinases and was positioned just downstream of the coding region within a highly conserved stretch (3′-primer used in RT-PCR reaction: 5′ CCCTAGTTTATTTCAGCATCAGC). The RT-PCR reaction yielded a single product of the expected size, which was subsequently cloned into a TOPO-TA cloning vector (Invitrogen, Carlsbad, CA). Plasmid DNA of several independent colonies was analysed by automated DNA sequencing. The resulting DNA sequence yielded a single open reading frame of 1143 base pairs with a translated amino-acid sequence of 381 amino acids. Database searches confirmed that the deduced protein is a new member of the cytosolic brain-type creatine kinase family.

2.9. Superposition of CK isoenzymes

Superpositions were performed using *LSQMAN* (Kleywegt, 1996) and *O* (Jones *et al.*, 1991).

3. Results and discussion

3.1. Structure of brB-CK subunit

The structure of the brB-CK subunit comprises two well defined domains (Fig. 1) with a fold very similar to previously solved structures of other CK isoenzymes (chicken mitochondrial Mi-CK; Fritz-Wolf *et al.*, 1996; PDB code 1crk), cytosolic rabbit muscle-type rM-CK (Rao *et al.*, 1998; PDB code 2crk), cytosolic chicken brain-type chB-CK (Eder *et al.*, 1999; PDB code 1qh4), human ubiquitous mitochondrial CK (uMi-CK; Eder *et al.*, 2000; PDB code 1qk1) and horseshoe crab arginine kinase hc-AK (Zhou *et al.*, 1998; PDB code 1qk1). The small lobe consists of N-terminal helices $\alpha1$–$\alpha6$ with their connecting loops and helix $\alpha9$; the larger domain comprises an eight-stranded antiparallel β-sheet enclosed by seven α-helices. Helices $\alpha10$ and $\alpha13$ from the large domain are positioned on one side of the β sheet; helices $\alpha11$, $\alpha12$ and $\alpha13$ cluster at one end of the β-sheet and helices $\alpha7$ and $\alpha8$ at the opposite end.

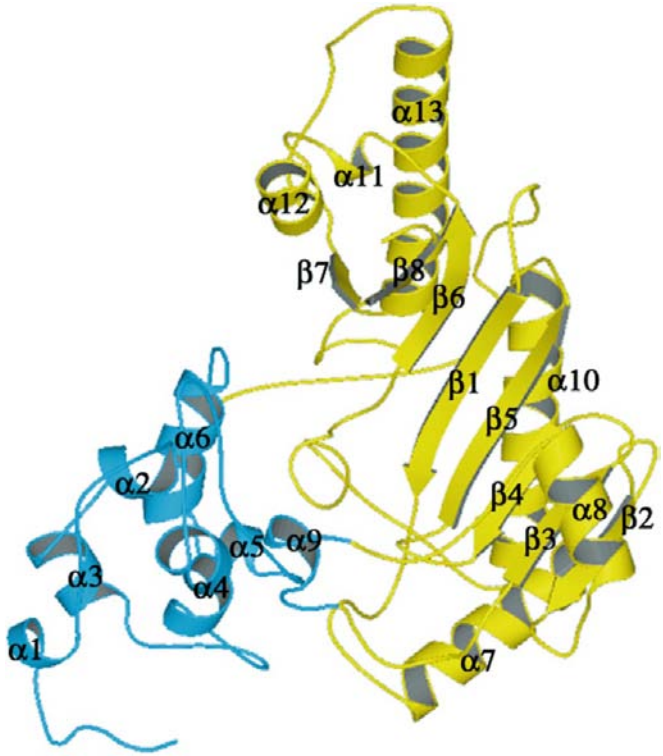

Figure 1
Ribbon representation of the structure of brB-CK. Secondary-structure elements were calculated using *PROCHECK* (Laskowski *et al.*, 1993). The small domain is shown in blue and the large domain is shown in yellow. Note that we have assigned helix $\alpha9$ as part of the small domain.

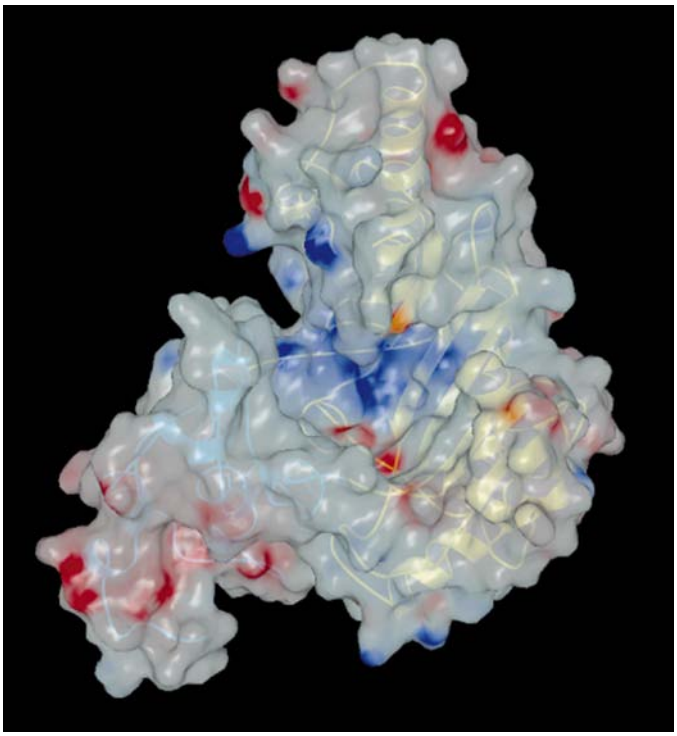

Figure 2
Electrostatic surface representation of brB-CK calculated in *GRASP* (Nicholls *et al.*, 1991). The active site of the enzyme between the two domains shows a strong positive surface (depicted in blue) resulting from the presence of a number of highly conserved arginine residues.

Analysis of those residues previously implicated in substrate binding or catalysis identified the location of the active site in a cleft between the large and small domains (Fritz-Wolf *et al.*, 1996; Zhou *et al.*, 2000; Eder *et al.*, 1999). This is enclosed on one side by strands β1, β5 and β6 (large domain) and on the other side by the loop region Met70–Asp79 (small domain) connecting helices α4 and α5. The active-site cleft is formed by helices α9 and α6. Helix α9 is positioned away from the large domain towards the small domain by two long loop regions and we suggest this helix is really part of the small domain. Helix α6 of the small domain and its following loop region are angled away from the small domain towards the large domain and the subsequent loop connects the small domain to the large domain.

Analysis of the electrostatic surface potential of the brB-CK monomer (Fig. 2) indicates a strongly positive region in the cleft between the two domains, which is likely to be the location of the nucleotide-binding site. Closer analysis of this region identified a cluster of several arginine residues with side chains located close to or pointing into the active-site cleft. Further analysis of this arginine cluster during refinement and rebuilding highlighted the presence of continuous density from the side chains of Arg130 and Arg320 to two regions of spherical density. Owing to the high concentration of ammonium sulfate present in the crystallization buffer, two sulfate groups were built into this density (Fig. 3).

3.2. The brB-CK dimer

The cytosolic CK isoenzymes function as dimers, unlike the mitochondrial isoenzymes which exist as octamers. The crystal structure of brB-CK contains a dimer with two protomers related by a twofold rotation axis (Fig. 4).

Four regions on each monomer contribute to the dimer interface (Fig. 4). (i) The N-terminal helix α1 forms several electrostatic interactions with the N-terminal end of helix α7 of the large domain from the second protomer. (ii) Residues of helix α4 (residues 54–62) of the small domain interact with a loop region (Met207–Asp210) of the large domain of the second protomer. (iii) The loop region Met207–Asp210 from the large domain of protomer one interacts with helix α4 of the small domain from the second protomer. (iv) The N-terminal region of α7 from the large domain of protomer one interacts with α1 from the small domain of protomer two. Residues involved in bonding at the dimer interface are summarized in Table 2.

Similar to the structure of cytosolic chicken brain-type creatine kinase (Eder *et al.*, 1999), we also observe alternate conformations at the N-terminus of each molecule of the homodimer. This is the second case where different N-terminal conformations of a homodimeric cytosolic brain-type creatine kinase have been found. However, it is still unclear if this feature is unique to brain-type CKs or is a general property of cytosolic creatine kinase, since in the structure of rabbit rM CK the N-terminus was disordered and was not included in the final coordinates (Rao *et al.*, 1998).

3.3. Comparison of brB-CK with other CK isoenzymes

Over the past few years several structures of CK isoenzymes have been made available and isoenzyme-specific structures can now be compared. As can be seen in the sequence alignment (Fig. 5), isoenzyme-specific sequence stretches are localized at the N-terminus, the linker region between the two domains, part of α-helix 10, α-helix 11 and 12 and at the C-terminus. With the exception of the N-terminus, the other

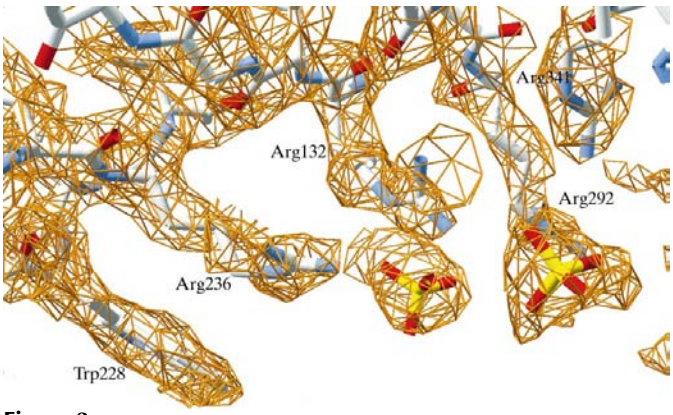

Figure 3
Structure of brB-CK highlighting active-site residues. Electron density of the final $2F_o - F_c$ map at a σ level of 1.0 is superposed on selected residues within the active-site cleft. Also shown are the sulfate ions originating from the ammonium sulfate present in the crystallization buffer. The picture was generated in *Swiss-PDB Viewer* (Guex & Peitsch, 1997) and rendered in *POV-Ray* (http://www.povray.org).

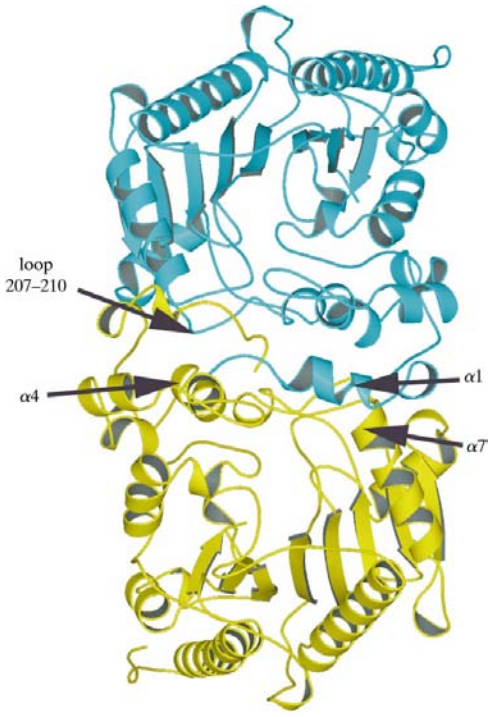

Figure 4
Structure of the brB-CK dimer. The dimer is composed of two monomers related by a twofold rotation axis (perpendicular to the plane of the paper). The dimer interface is formed mainly by four regions (α1/α7 and loop207–210/α4) as described in detail in the text. The first 11 amino acids of each monomer are tentatively build into density with an occupancy of 0.5.

Table 2
Contacts at the dimer interfaces in brB-CK and chicken mitochondrial creatine kinase (cMi-CK; PDB code 1crk).

For cMi-CK, contacts between the *C* and *C*′ subunits round the crystallographic twofold are listed; similar contacts exist between the *A* and *B*′, *B* and *A*′ and *D* and *D*′ subunits). All contacts <3.3 Å between a hydrogen-bond donor and a hydrogen-bond acceptor are listed (waters at the dimer interface have not been included).

brB-CK			cMi-CK (*C* to *C*′ subunit)		
Subunit 1	Distance (Å)	Subunit 2	Subunit 1	Distance (Å)	Subunit 2
Asn8 ND2	3.07	His145 O			
Asn8 ND2	3.08	Glu150 OE1			
Thr9 N	3.13	Ser49 O			
Thr9 OG1	2.82	Pro48 O			
Asp18 O	2.91	Arg152 NH1			
Glu19 OE2	2.67	Ser147 OG	Asp14 OD1	3.26	Ser142 OG1
Glu19 OE1	2.93	Gly149 N	Asp14 OD1	3.04	Ala144 N
Glu19 OE1	3.29	Arg148 N			
Glu19 O	2.70	Arg148 NE			
Glu19 O	3.12	Arg148 NH1	Asp14 O	2.61	Arg143 NH1
Phe20 O	2.74	Arg152 NH1	Tyr15 O	2.59	Arg147 NH2
Phe20 O	3.02	Arg152 NH2			
Asp22 OD2	2.39	Lys177 NZ			
			Lys20 NZ	2.95	Asn173 OD1
Asp54 OD1	2.80	Arg148 NH1	Asp49 OD1	3.16	Arg143 NH2
Gln58 NE2	2.98	Asp210 OD1	Gln53 NE2	2.76	Asp205 OD1
Asp62 OD1	2.78	Asp210 N	Asp57 OD1	2.57	Asp205 N

stretches of divergent sequence display a conserved three-dimensional structure. Their differences result only in electrostatic changes at the surface of the protein. It appears however that the N-terminus displays a quite unique three-dimensional isoenzyme-specific structure important in dimer formation in both the cytosolic brain-type forms thus far solved (Eder *et al.*, 1999 and present paper) as well as for octamer formation of the mitochondrial forms (Fritz-Wolf *et al.*, 1996; Eder *et al.*, 2000). This unique feature might explain its larger degree of variation compared with the rest of the protein sequence. [The only structure of a muscle-type isoenzyme available (Rao *et al.*, 1998) is lacking the first seven N-terminal amino acids.]

Least-squares superposition of a monomer of brB-CK with cMi-CK results in an r.m.s. difference of only 0.91 Å (for all C^{α} backbone atoms excluding the N-terminus, a total of 359 atoms). Comparison with uMi-CK yields very similar results (0.79 Å for the monomer, a total of 358 atoms).

Superposition of the two brain-type isoenzymes brB-CK with chB-CK yields an r.m.s. difference of 0.8 Å for a total of 358 atoms. Surprisingly, the smallest r.m.s. difference is observed when comparing brB-CK and rabbit muscle rM-CK. Their least-squares superposition results in an overall r.m.s. difference of only 0.76 Å for the monomer (a total of 360 C^{α} atoms). Further comparison with the high-resolution chicken brain-type structure (Eder *et al.*, 1999) again confirmed the presence of the *cis* proline bond at position 212. This *cis* proline appears to be conserved throughout all the CK isoenzymes and has also been found in the transition-state structure of arginine kinase (Zhou *et al.*, 1998). In addition, as in the structure of chB-CK, the unusual backbone geometry of the highly conserved Glu231 is also preserved in brB-CK, suggesting a more prominent role for Glu231 in catalysis (Eder *et al.*, 1999).

The active site of creatine kinase contains a cluster of highly conserved arginines (Arg96, 130, 132, 135, 236, 292 and 320). Comparison with the previously solved structures of chicken mitochondrial CK (cMi-CK) complexed with ATP (Fritz-Wolf *et al.*, 1996) and the transition-state structure of arginine kinase (Zhou *et al.*, 1998) suggested these arginines to be involved in binding of the phosphate groups of the adenine nucleotide. Owing to the high ammonium sulfate content of the crystallization buffer, two well

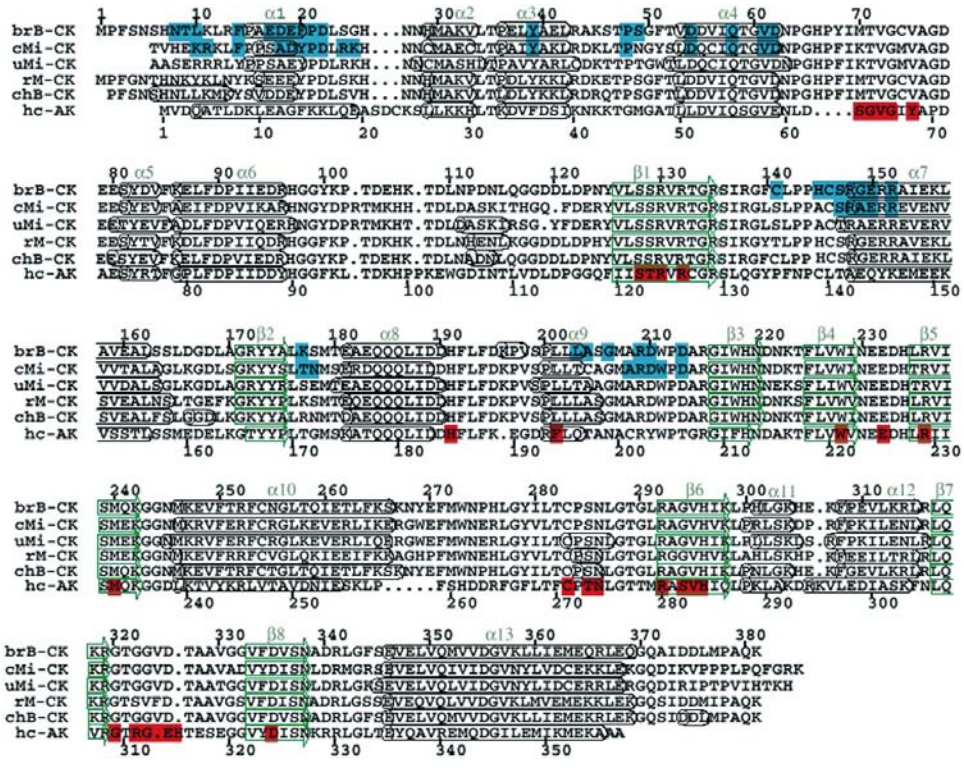

Figure 5
Alignment of sequences of bovine retinal brain-type creatine kinase (brB-CK), chicken mitochondrial CK (cMi-CK), human ubiquitous mitochondrial CK (uMi-CK), rabbit muscle CK (rM-CK), chicken brain-type CK (chB-CK) and horseshoe crab arginine kinase (hc-AK). α-Helices are represented as cylinders and β-strands are shown as green arrows. Highlighted in blue are residues making contacts across the brB-CK and the cMi-CK dimer interface (distances less than 4 Å). Residues in red are amino acids with distances less then 4 Å of transition-state analogue substrate in horseshoe crab arginine kinase.

defined sulfate ions are present in the active site in the approximate position of the corresponding α- and γ-phosphates of the nucleotides in the structures of cMi-CK and hc-AK. These sulfate ions appear to stabilize the conformations of the conserved arginines, leading to well ordered side chains. Both sulfates have also been observed at very similar positions in the structure of rabbit muscle-type CK (Rao *et al.*, 1998). However, a third sulfate ion near the conserved Cys283 as observed in rM-CK is not present in the structure of brB-CK.

4. Summary

The maintenance of cellular energy levels is critical to the survival of all cells. Cells with fluctuating levels of ATP, such as muscle cells, are solely dependent on creatine kinase isoforms and the associated phosphocreatine shuttle system to synthesize ATP and maintain energy homeostasis.

The crystal structure of the dimeric cytosolic isoform of bovine retinal brain-type creatine kinase has provided a further dimension to the investigation of the mechanism of catalysis of this critical enzyme as well as isoenzyme-specific differences.

The authors would like to thank Dr Judith Murray-Rust for critical reading of the manuscript and Dr Anette Huebner for advice in cloning and sequencing of the bovine retinal creatine kinase gene.

References

Belousova, L.V., Fedosov, S. N., Orlova, E. V. & Stel'mashchuk, U. Y. (1991). *Biochem. Int.* **24**, 51–58.
Beutner, G., Ruck, A., Riede, B., Welte, W. & Bridiczka, D. (1996). *FEBS Lett.* **396**, 189–195.
Borders, C. L. & Riordan, J. F. (1975). *Biochemistry*, **14**, 4699–4704.
Bose, S. & Friedberg, F. (1971). *Biochem. Biophys. Res. Commun.* **45**, 271–277.
Brunger, A. T., Adams, P. D., Clore, G. M., Gros, P., Grosse-Kunstleve, R. W., Jiang, J.-S., Kuszewski, J., Nilges, M., Pannu, N. S., Read, R. J., Rice, L. M., Simonson, T. & Warren, G. L. (1998). *Acta Cryst.* D**54**, 905–921.
Buechter, D. D., Medzihtadszky, K. F., Burlingame, A. L. & Kenyon, G. L. (1992). *J. Biol. Chem.* **267**, 2173–2178.
Collaborative Computational Project, Number 4 (1994). *Acta Cryst.* D**50**, 760–763.
DeLuca, M. & Hall, N. (1980). *Heart Creatine Kinase*, edited by W. E. Jacobus & J. S. Ingwall, pp. 18–27. Baltimore/London: Williams & Wilkins.
Eder, M., Fritz-Wolf, K., Kabsch, W., Wallimann, T. & Schlattner, U. (2000). *Proteins*, **39**(3), 216–225.
Eder, M., Schlattner, U., Becker, A., Wallimann, T., Kabsch, W. & Fritz-Wolf, K. (1999). *Protein Sci.* **8**, 2258–2269.
Ellington, W. R. (1989). *J. Exp. Biol.* **143**, 177–194.
Eppenberger, H. M., Dauson, D. M & Kaplan, N. O. (1967). *J. Biol. Chem.* **242**, 204–209.
Forstner, M., Kriechbaum, M., Laggner, P. & Walliman, T. (1996). *J. Mol. Struct.* **383**, 217–222.
Fritz-Wolf, K., Schnyder, T., Walliman, T. & Kabsch, W. (1996). *Nature (London)*, **381**, 341–345.
Furter, R., Furter-Braves, E. M. & Walliman, T. (1993). *Biochemistry*, **32**, 11935–11941.
Gross, M., Furter-Graves, E. M., Wallimann, T., Eppenberger, H. M. & Furter, R. (1994). *Protein Sci.* **3**, 1058–1068.
Guex, N. & Peitsch, M. C. (1997). *Electrophoresis*, **18**, 2714–2723.
Hossle, J. P., Schlegel, J., Wegmann, G., Wyss, M., Bohlen, P., Epenberger, H. M., Wallimann, T. & Perriard, J. C. (1988). *Biochem. Biophys. Res. Commun.* **151**, 408–416.
Jacobus, W. E. & Lehninger, A. L. (1973). *J. Biol. Chem.* **248**, 4803–4810.
James, T. L. & Cohn, M. (1974). *J. Biol. Chem.* **249**, 2599–2604.
Jones, T. A., Zou, J. Y., Cowan, S. W. & Kjeldgaard, M. (1991). *Acta Cryst.* A**47**, 110–119.
Kleywegt, G. J. (1996). *Acta Cryst.* D**52**, 842–857.
Laskowski, R. A., MacArthur, M. W., Moss, D. S. & Thornton, J. M. (1993). *J. Appl. Cryst.* **26**, 283–291.
Lehninger, A. L. (1992). *Principles of Biochemistry*, 2nd ed. New York: Worth.
Loew, A. & Bax, B. (1998). *Acta Cryst.* D**54**, 989–990.
Muhlebach, S. M., Gross, M., Wirz, T., Walliman, T., Perriard, J. C. & Wyss, M. (1994). *Mol. Cell. Biochem.* **133**/**134**, 245–263.
Murshudov, G. N., Vagin, A. A., Lebedev, A., Wilson, K. S. & Dodson, E. J. (1999). *Acta Cryst.* D**55**, 247–255.
Navaza, J. & Saludjian, P. (1997). *Methods Enzymol.* **276**, 581–593.
Nicholls, A., Sharp, K. A. & Honig, B. J. (1991). *Proteins*, **11**, 218–296.
Otwinowski, Z. & Minor, W. (1997). *Methods Enzymol.* **276**, 307–326.
Perrakis, A., Morris, R. & Lamzin, V. S. (1999). *Nature Struct. Biol.* **6**, 458–463.
Rao, J. K., Bujacz, G. & Wlodawer, A. (1998). *FEBS Lett.* **439**(1–2), 133–137.
Schlegel, J., Zurbriggen, B., Wegmann, G., Wyss, M., Eppenberger, H. M. & Walliman, T. (1988). *J. Biol. Chem.* **263**, 16942–16962.
Vasak, M., Nagayama, K., Wuthrich, K., Mertens, M. L. & Kagi, J. H. R. (1979). *Biochemistry*, **18**, 5050–5055.
Wallimann, T., Schlosser, T. & Eppenberger, H. M. (1984). *J. Biol. Chem.* **259**, 5238–5246.
Wallimann, T., Wyss, M., Brdiczka, D., Nicolay, K. & Eppenberger, H. M. (1992). *Biochem. J.* **281**, 21–40.
Watts, D. C. (1971). *Biochemical Evolution and the Origin of Life*, edited by E. Schffieniel, pp. 150–173. Amsterdam: North Holland.
Watts, D. C. (1973). *The Enzymes*, edited by P. D. Boyer, Vol. 8, pp. 388–455. New York: Academic Press.
Wegmann, G., Zanolla, E., Eppenberger, H. M. & Walliman, T. (1992). *J. Muscle Res. Cell. Motil.* **13**, 420–435.
Wood, T. D., Guan, Z., Borders, C. L., Chen, L. H., Kenyon, G. L. & McLafferty, F. W. (1998). *Proc. Natl Acad. Sci. USA*, **95**, 3362–3365.
Zhou, G., Ellington, W. R. & Chapman, M. S. (2000). *Biophys. J.* **78**(3), 1541–1550.
Zhou, G., Thayumanasamy, S., Blanc, E., Golapakrishnan, P., Ellington, W. R. & Chapman, M. S. (1998). *Proc. Natl Acad. Sci. USA*, **95**, 8449–8454.